Oxidation barrier of Cu and Fe powder by Atomic Layer Deposition

Oxidation barrier of Cu and Fe powder by Atomic Layer Deposition

Véronique Cremers[a], Geert Rampelberg[a], Ahmed Barhoum[b], Perry Walters[b], Nathalie Claes[d], Thais Milagres de Oliveira[d], Guy Van Assche[c], Sara Bals[d], Jolien Dendooven[a], Christophe Detavernier[a]

[a]Department of Solid State Sciences, Ghent University, Krijgslaan 281/S1, B-9000 Ghent, Belgium

[b]Chemistry Department, Faculty of Science, Helwan University, Cairo 11795, Egypt

[c]Physical Chemistry and Polymer Science, Vrije Universiteit Brussel (VUB), Pleinlaan 2, 1050 Brussels, Belgium

[d]Electron Microscopy for Materials Research (EMAT), University of Antwerp, Groenenborgerlaan 171, Antwerp 2020, Belgium

Highlights

- Pinhole free, uniform and conformal oxidation barrier on Cu and Fe powder.
- Proper agitation of the powder is required and performed by a rotating ALD reactor.
- Al2O3 coating of 8 nm on Cu powder causes a shift of oxidation temperature of 200 °C
- Al2O3 coating of 25 nm on Fe powder causes a shift of oxidation temperature of 400 °C

Abstract

Atomic layer deposition (ALD) is a vapor based technique which allows to deposit uniform, conformal films with a thickness control at the atomic scale. In this research, Al_2O_3 coatings were deposited on micrometer-sized Fe and Cu powder (particles) using the thermal trimethylaluminum (TMA)/ water (H_2O) process in a rotary pump-type ALD reactor. Rotation of the powder during deposition was required to obtain a pinhole-free ALD coating. The protective nature of the coating was evaluated by quantifying its effectiveness in protecting the metal particles during oxidative annealing treatments. The Al_2O_3 coated powders were annealed in ambient air while in-situ thermogravimetric analysis (TGA) and in-situ x-ray diffraction (XRD) data were acquired. The thermal stability of a series of Cu and Fe powder with different Al_2O_3 thicknesses were determined with TGA. In both samples a clear shift in oxidation temperature is visible. For Cu and Fe powder coated with 25 nm Al_2O_3, we observed an increase of the oxidation temperature with 300-400°C. For the Cu powder a thin film of only 8 nm is required to obtain an initial increase in oxidation temperature of 200°C. In contrast, for Fe powder a thicker coating of 25 nm is required. In both cases, the oxidation temperature increases with increasing thickness of the Al_2O_3 coating. These results illustrate that the Al_2O_3 thin film, deposited by the thermal ALD process (TMA/H_2O) can be an efficient and pinhole-free barrier layer for micrometer-sized powder particles, provided that the powder is properly agitated during the process to ensure sufficient vapour-solid interaction.

Keywords

Atomic Layer Deposition; ALD; Powder; Oxidation barrier

1. Introduction

To prevent metal surfaces from oxidation, different coating methods have been studied as plasma spraying [[1]; [2] ; [3]], and sputtering [4, 5]. However these methods have only a limited thickness control of the coating. In recent years, Atomic Layer Deposition (ALD) is increasingly investigated for the surface functionalization of powders [6]. ALD is a gas-phase deposition technique which allows to deposit layer-by-layer thin films with an excellent control of thickness at the atomic scale [[7]; [8]; [9]; [10]; [11] ; [12]]. Due to the self-limited nature of the chemical reactions, ALD enables to grow uniform and conformal thin films even in high aspect ratio [13] or porous structures [14, 15]. Powder ALD has been explored for the encapsulation of moisture sensitive powder [16], catalytic activation [17], improving the powder rheology and preventing the powder to oxidize [18]. Hakim et al. [19] studied the coating of nano-iron particles with Al2O3 in order to prevent the oxidation of the powder. To overcome the thermal expansion mismatch between the iron particle and the Al2O3 coating, Moghtaderei et al. [20] studied the coating barrier of alternating layers of Al2O3/ZnS which has similar thermal properties as the iron substrate. Most studies so far were performed in fluidized-bed reactors [21].

In this research we aim to deposit uniform, conformal and pinhole-free coatings of Al2O3 on micron-sized Cu and Fe powder, using a pump-type rotary ALD reactor, to protect these powders against oxidation. We will investigate the effect of the thickness of the coating (6-30nm) and the substrate (Cu or Fe powder) on the barrier properties of the coating.

2. Experimental

Contrary to the often used fluidized bed reactors, [22] the ALD depositions took place in a home-built pump-type rotary ALD reactor for powders [23, 24]. The reactor contains a rotating quartz tube in which a cylindrical stainless steel container is placed, containing the powder. The front and the back of the container is a membrane which allows the precursor/reactant gas to flow through the container and react with the powder while the powder is forced to stay in the container. The rotation permits the mechanical agitation of the powder which is required for a conformal coating. The aluminum oxide films were deposited by using trimethylaluminum (TMA, 97 %, Sigma-Aldrich) and H2O as precursor and reactant respectively. Both were stored in a stainless steel bottle at room temperature. The precursor lines were heated to 50°C and the temperature of the powder sample was kept at 100°C. One ALD cycle consisted of a pulse time of 20 s of TMA followed by a pump-time of 60 s, a pulse time of 20 s of H2O and a pump-time of 60 s. A metering valve regulated the flow of the precursor/reactant to the reactor resulting in a partial pressure of

2.10−3 mbar and 3.10−3 mbar for TMA and H2O respectively. The base pressure in the reactor during the process was maintained at 1.10−5 mbar. During this research, Cu and Fe powder were studied with an average particle size of <45 µm and ~ 325 mesh respectively (Sigma Aldrich). The Fe particles have random shapes and the Cu particles have a dendritic structure.

The presence of the deposited alumina coating was measured using a FEI Quanta 200 F Scanning Electron Microscope (SEM) and Energy Dispersive X-ray spectroscopy (EDX) with the electron beam energy set at 15 keV. Transmission Electron Microscopy (TEM) was used to visualize the deposited coating and to investigate the conformality and the thickness of the coating. In high angle annular dark field scanning transmission microscopy (HAADF-STEM), the intensity is proportional to Z2 with Z the atomic number. This allows to distinguish the core materials from the coating. Because of the magnetic properties of the Fe powder an extra step in the sample preparation for STEM analysis was needed. First, the Fe particles were crushed in a solution of ethanol. Then, the solution of ethanol and crushed Fe particles was deposited on the TEM grid. A strong magnet was used to remove the excess of Fe particles.

Besides investigating the characteristics of the coating, the capacity of the alumina coating for protecting the powder against oxidation was investigated. Thermogravimetric analysis (TGA) and in-situ x-ray diffraction (XRD) were used to study the thermal stability and oxidation properties of the coated powder during anneals. The in-situ XRD measurements were performed in a home-built setup [[25]; [26]; [27] ; [28]] in ambient air with a ramp rate of 10 K/min. A Cu Kα X-ray source and a position sensitive detector were used to obtain the XRD patterns. The TGA measurements were performed using a TGA Q5000 IR (TA Instruments, USA) on 10 mg of powder which was placed in platinum pans. First, there was an initial isothermal at 60°C, followed by an anneal in air till 850°C with a heating rate of 10K/min. After the anneal, the temperature was lowered to 60°C at 10K/min to determine the weight change defined as the change in mass of the sample between start- and end point. Out of the TGA measurements, one can derive the oxidation temperature which is defined as the lowest temperature where mass increase due to oxidation is observed.

3. Results and discussion

Fig. 1 shows the SEM image and EDX measurement of the dendritic Cu powder coated with 150 ALD cycles of TMA/H2O. The Cu particles vary in size and have an inhomogenous dendritic structure. In the EDX spectrum a clear Al Kα peak is observed at 1.486 keV, indicating the presence of the Al2O3 coating. The C signal originates from the C-tape on which the powder is positioned during the measurements.

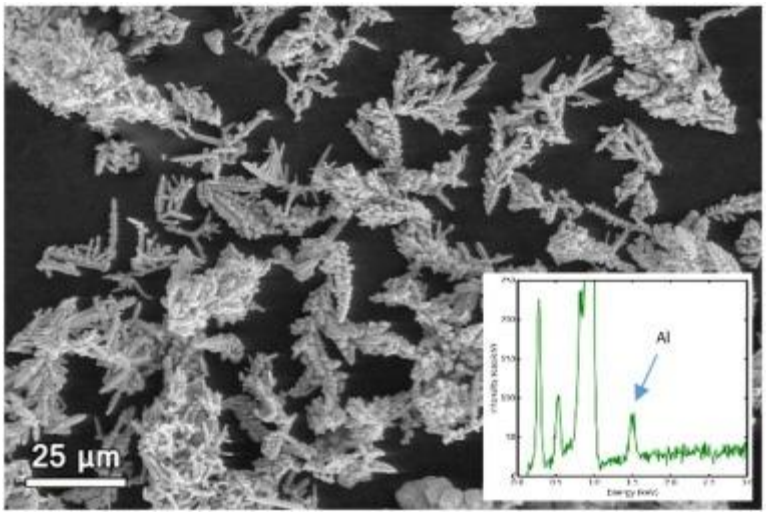

Fig. 1. SEM images of the dendritic Cu powder coated with 150 cycles of TMA/H2O. The inset figure show the EDX spectrum.

TEM measurements were performed to investigate the conformality, uniformity and thickness of the coating. Fig. 2 shows the TEM images of a Cu particle coated with 150 ALD cycles. The EDX analysis shows a surrounding layer containing Al and O. From STEM imaging, one can estimate the film thickness to be 15 nm, corresponding with a growth rate of 0.1 nm per cycle. This is in reasonable agreement with the growth rate of 0.13 nm per cycle of the process under similar process conditions, found in literature [29]. This result illustrates the characteristic control of the film thickness which is typical for ALD processes. By combining STEM imaging with different tilt angles and XEDS analysis, one can observe that the coating is uniform and conformal along the entire particle.

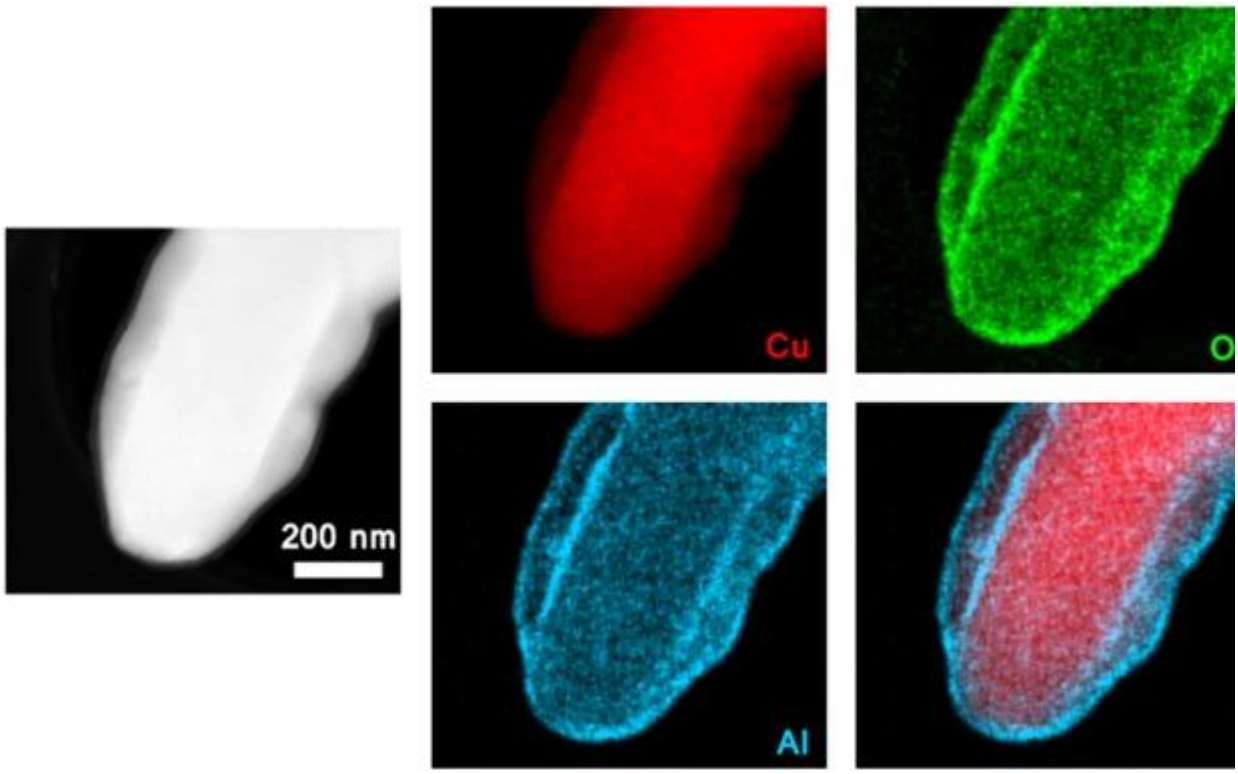

Fig. 2. HAADF-STEM images and EDX mapping results of a Cu particle, coated with 150 ALD cycles.

Fig. 3 shows an EDX line profile analysis along the line showed in the HAADF-STEM image of a Cu particle coated with 150 ALD cycles. Outside the particle, when the Cu signal is low, we observe strong O and Al signals which decrease while the Cu signal increases, indicating that the Al2O3 coating is only on the outside of the particle.

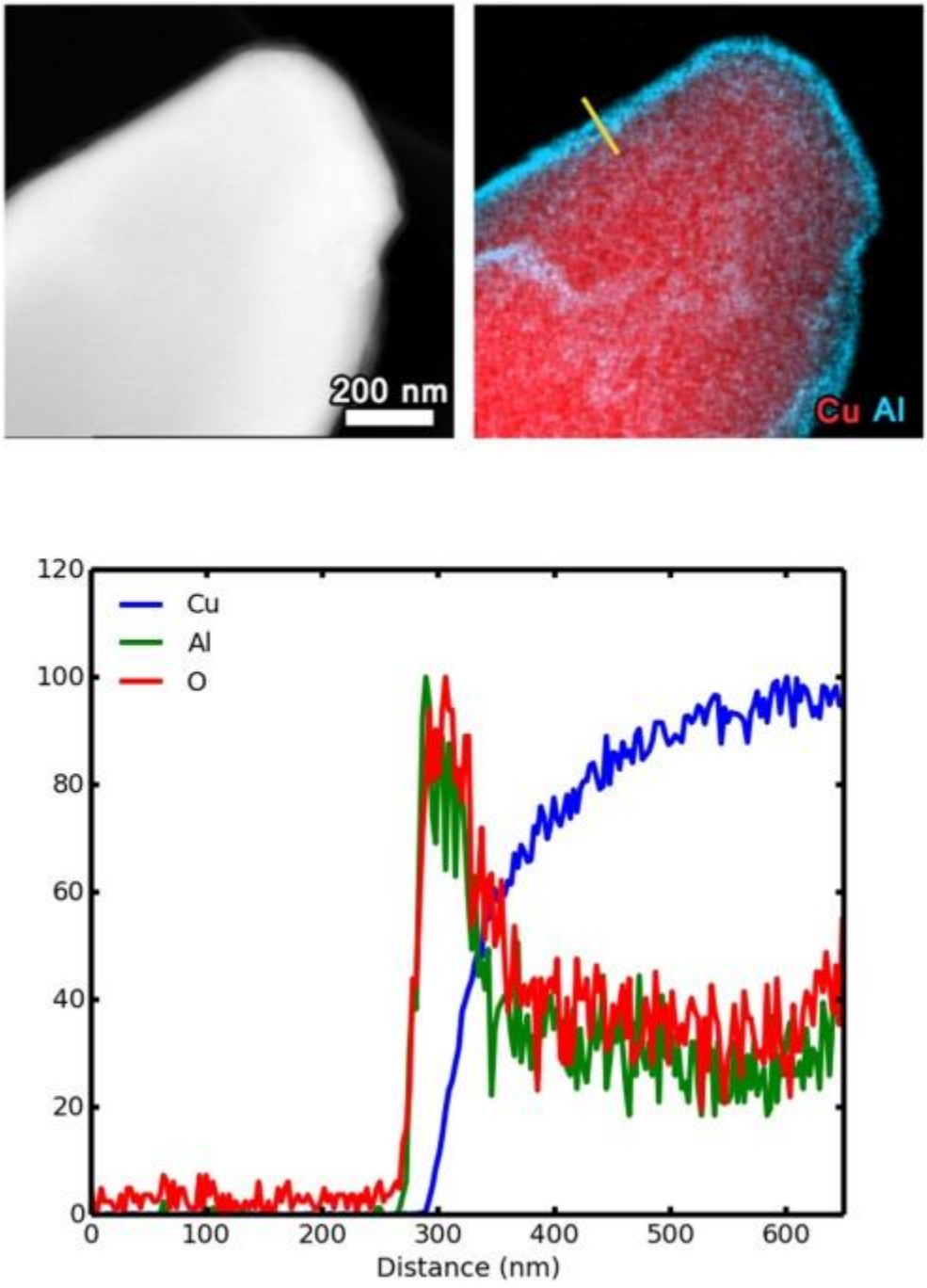

Fig. 3. Line Profile analysis of the coated Cu powder (150 ALD cycles).

Previous measurements indicate the presence of an uniform and conformal Al2O3 coating. To explore the pinhole-free nature of the coating, the protective barrier property of the coating against oxidation was studied with in-situ XRD and TGA measurements during an anneal in ambient air. To investigate the effect of mechanical agitation of the powder during deposition on the quality of the coating, Cu powder was coated with 150 ALD cycles under stationary conditions and while the reactor containing the powder was rotating at 37 rpm during the entire ALD process, keeping all other process conditions identical. Fig. 4 shows the in-situ XRD patterns during an anneal in ambient air of an uncoated Cu sample (a) compared with a Cu sample coated with 150 ALD cycles in a stationary reactor (i.e. without rotation) (b) and a Cu sample coated with 150 ALD cycles while the reactor was rotating to

ensure proper vapor-solid interation through agitation of the powder (c). The corresponding 2θ diffraction peaks are indicated in the figure. It is clearly seen that the Cu peaks remain present until much higher temperature for both coated samples ((b) and (c)) than for the uncoated sample. The Cu2O and CuO peaks appear at a much higher temperature for the coated sample with rotation (c) (300 degrees higher) than in case of the uncoated sample and the coated sample without rotation. Not only an increased oxidation temperature is observed for the coated sample with rotation, but one also observes that the region during which the Cu and the Cu2O and CuO phases coexist is much narrower in comparison with both other samples. The absence of rotation during deposition causes a decrease of the oxidation temperature of almost 150°C. This result shows that for the ALD process without rotation the major part of the powder is well coated and protected against oxidation, but the coating contains pinholes causing an earlier start of the oxidation. This experiment shows the necessity of agitating the powder during the ALD process to ensure proper vapor-solid interaction. All experiments discussed in the remainder of the paper were performed with rotation during the ALD process.

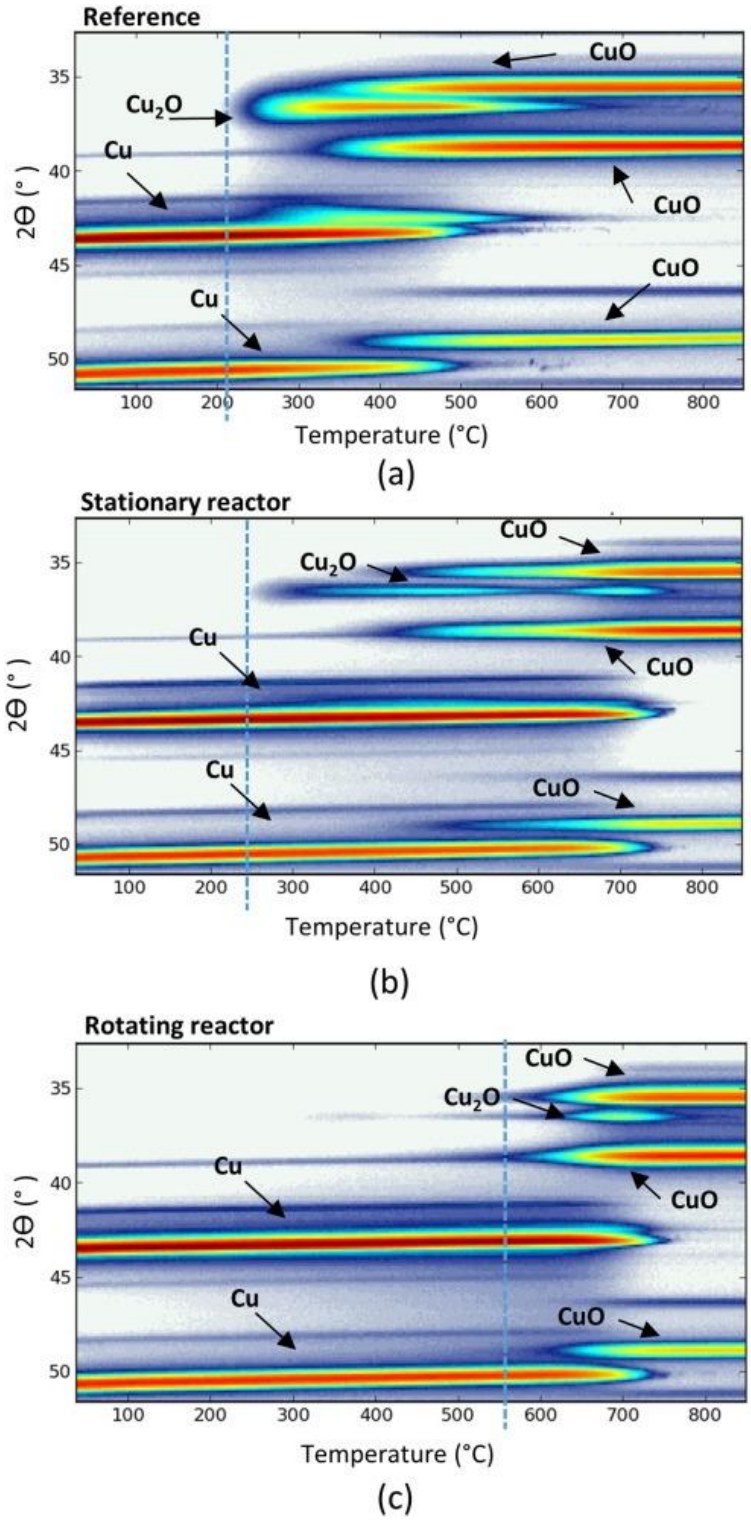

Fig. 4. In-situ XRD measurements of dendritic Cu powder during an anneal in ambient air (10K/min): uncoated reference (a), with an Al2O3-coating after 150 ALD cycles in a stationary reactor (i.e. without rotation resulting in a non-agitated powder bed) (b) and with an Al2O3-coating after 150 ALD cycles while the reactor was rotating at 37 rpm to ensure proper vapor-solid interaction through agitation of the powder (c).

Besides the Cu powder, Fe powder was also deposited with an alumina coating. Fig. 5 shows the SEM/EDX measurements of the Fe powder coated with 150 ALD cycles of TMA/H2O. The

Fe particles vary strongly in size and have a more spherical structure in comparison with the dendritical Cu particles. The EDX spectrum shows a clear peak at 1.486 keV, indicating the presence of the Al2O3 coating.

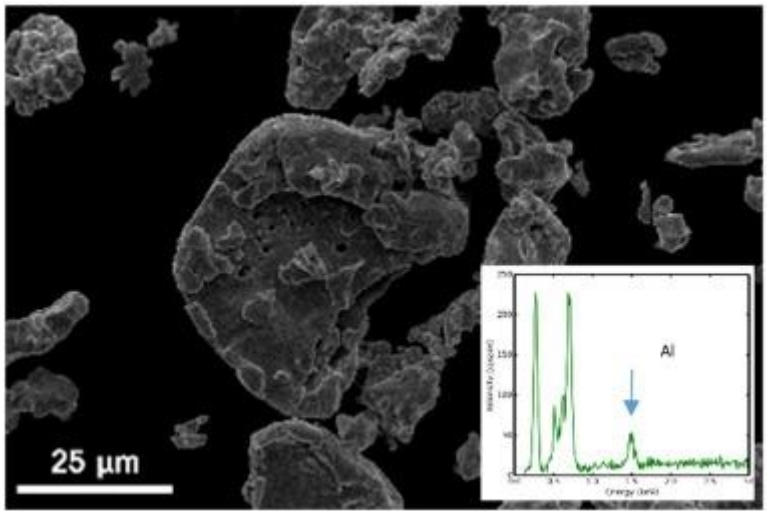

Fig. 5. SEM images of the Fe powder coated with 150 cycles of TMA/H2O. The inset figure show the EDX spectrum.

Fig. 6 shows the TEM images of a Fe particle coated with 150 ALD cycles. Similar to the results of the Cu powder, the EDX analysis shows a surrounding layer containing Al and O. Besides these elements, also Mn and Ca have been observed, probably originating from contamination of the blank powder sample. From STEM imaging, one can estimate a film thickness of 17 nm which is slightly higher than in case for the Cu powder, but still in line with the expected film thickness.

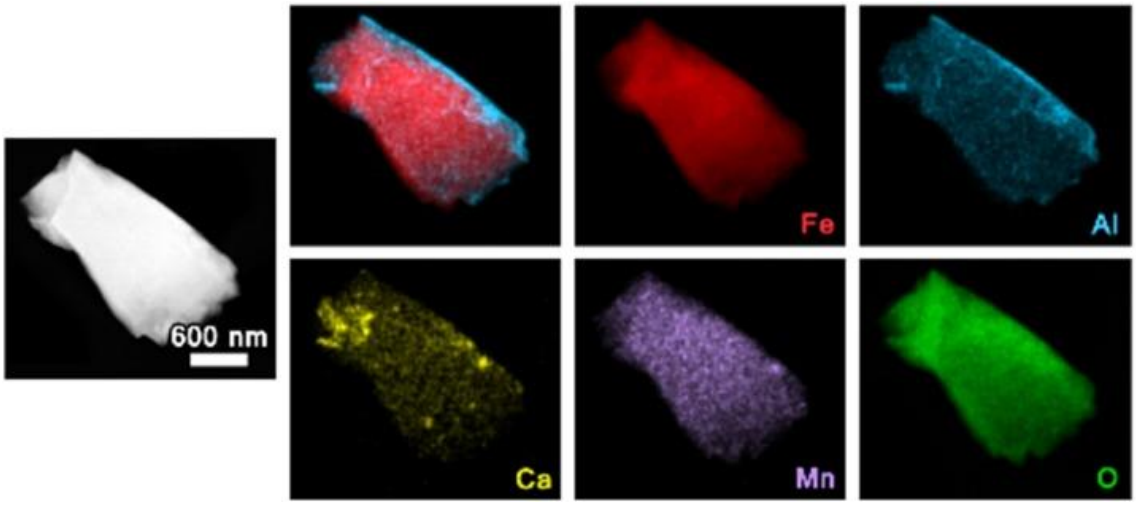

Fig. 6. HAADF-STEM images and EDX mapping results of a Fe particle, coated with 150 ALD cycles.

Fig. 7 shows the line profile analysis of a Fe particle coated with 250 ALD cycles. Similar to the profile of the Cu particle we observe a large Al signal when the Fe signal is low. The Al signal is slowly decreasing while the Fe signal increases.

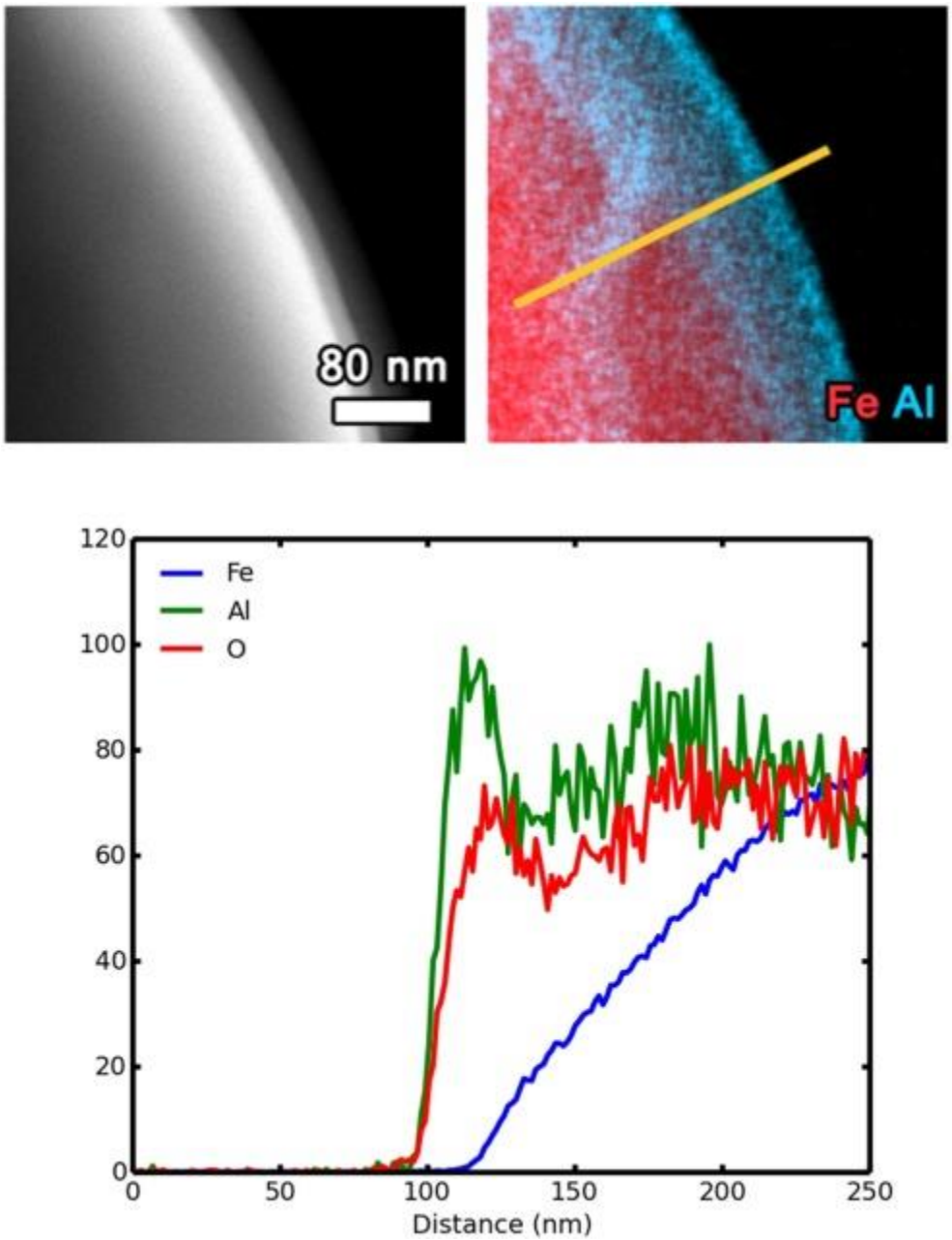

Fig. 7. Line Profile analysis of the coated Fe powder (250 ALD cycles).

To study the effect of coating thickness on the quality of the oxidation barrier, a series of depositions were performed with varying number of ALD cycles in the range of 60 to 300 cycles with a corresponding expected thickness in the range of 6-30 nm. To represent the data on the oxidation process in a more quantitative way, the integrated intensity of the Cu (2θ=43.298°) and the CuO (2θ=48.717°) diffraction peaks can be integrated in the in-situ XRD data. The integrated intensities for a series of samples with varying ALD cycles in the range of 0-250 is shown in Fig. 8. One observes that the slope of the increase/decrease of the integrated intensity is more or less similar for the different coating thicknesses, but that the onset of oxidation shifts with increasing coating thickness.

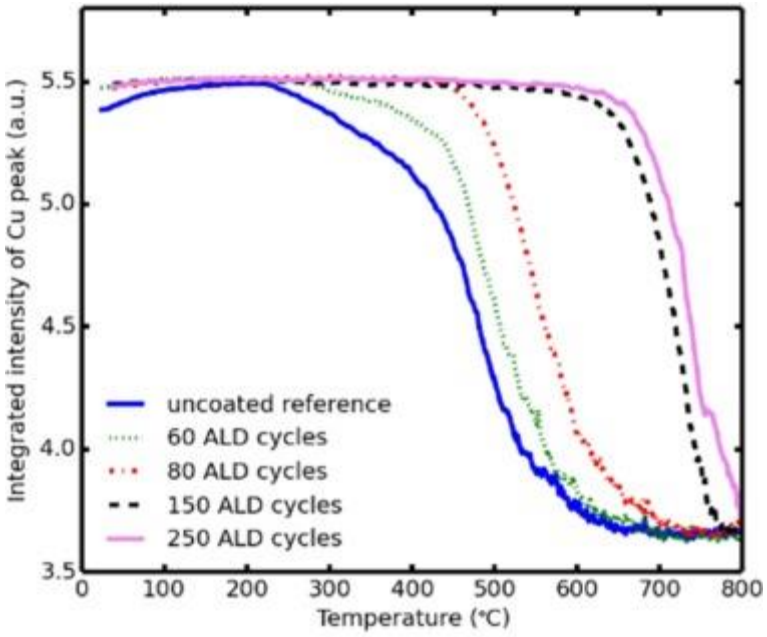

(a)

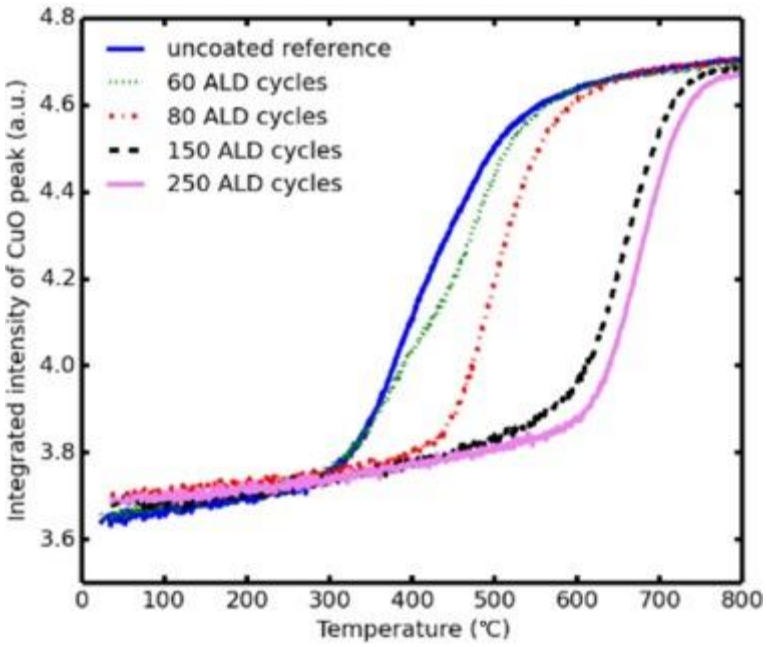

(b)

Fig. 8. Integrated intensity of the in-situ XRD measurements of the Cu peak (2θ=43.298°) (a) and the CuO peak (2θ=48.717°)(b), for a series of Cu powders coated with 0-250 ALD cycles in a rotary reactor.

Fig. 9 shows in-situ XRD data for the uncoated (a) and coated Fe powder with 150 ALD cycles (b). The difference in the two figures is less pronounced than in case of the Cu powder. The Fe and Fe2O3 XRD peaks are more overlapping which makes this technique not suitable to indentify the oxidation temperature of the Fe powder.

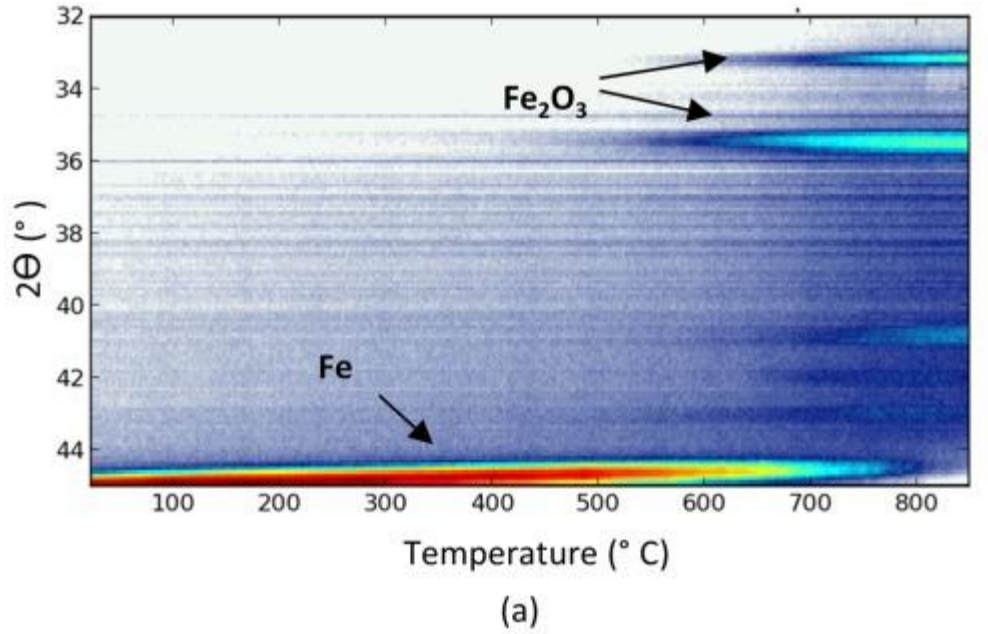

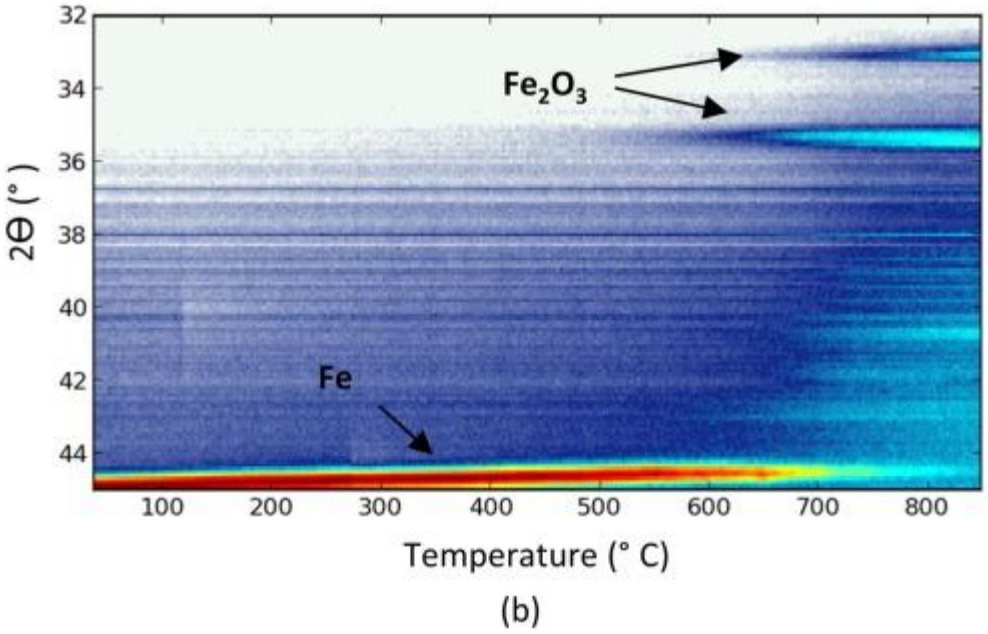

Fig. 9. In-situ XRD measurements of Fe powder: uncoated reference (a) and with an Al2O3-coating after 150 ALD cycles (b), during an anneal in ambient air (10K/min).

The oxidation temperature of the Fe and Cu powder samples was also quantified through TGA measurements. In Fig. 10 the TGA measurements are shown for a series of Cu (a) and Fe (b) samples with different coating thicknesses (0-300 ALD cycles), annealed at a rate of 10 K/min in ambient air. The TGA measurements confirm the result of the in-situ XRD measurements: the oxidation temperature increases with increasing coating thickness. For the Cu powder, a coating of 8 nm of alumina causes already a shift in oxidation temperature of 200°C, however for the Fe powder an alumina coating of 250 ALD cycles is required to cause an intial shift in oxidation temperature. The total increase of the weight percentage after the anneal was equal to 25 %. The in-situ XRD measurements indicate that the CuO phase is formed as the final phase. Because m(Cu) ≈ 4.m(O), we expect a mass increase of

25 % which is in agreement with the TGA results. Similar for the Fe powder, the in-situ XRD measurements showed the formation of Fe2O3. With m(Fe) ≈ 3,5.m(O) and taking into account the stoichiometry of the phase, we expect a mass increase in the range of 40%, which is in agreement with the TGA results. TGA permits also a precise quantification of the oxidation temperature, certainly in case of the Fe samples where in-situ XRD measurements could not give a clear result. To compare the quality of the alumina coating as an oxidation barrier for Cu and Fe powder, the oxidation temperature as determined from TGA measurements is plotted as a function of the expected coating thickness for the Cu and the Fe powder, in Fig. 11. We observe that for the Cu powder, an alumina coating of 8 nm causes already a large increase in oxidation temperature of 200°C, while for the Fe powder an alumina coating of 25 nm is needed to cause an initial shift in oxidation temperature of 250°C.

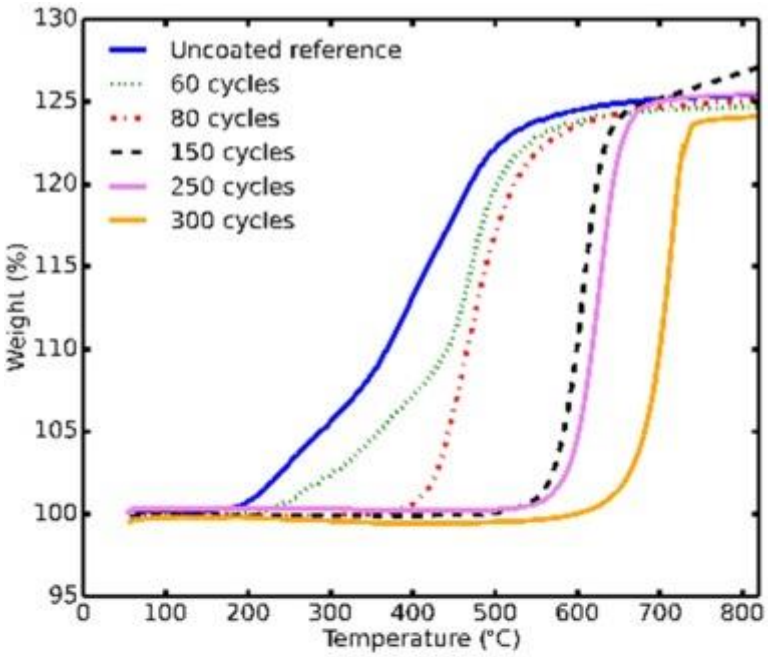

(a)

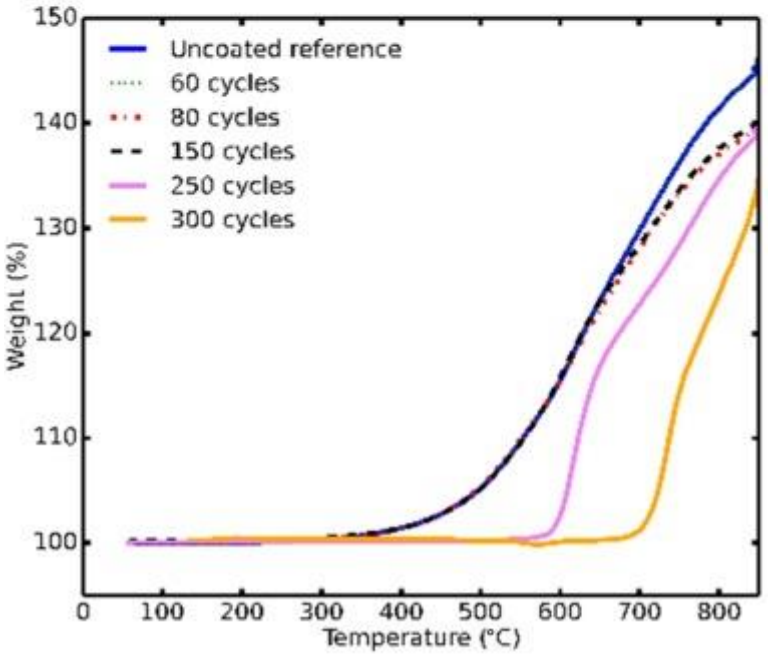

(b)

Fig. 10. TGA measurements of a series of Cu (a) and Fe (b) powder, coated with 0-300 ALD cycles.

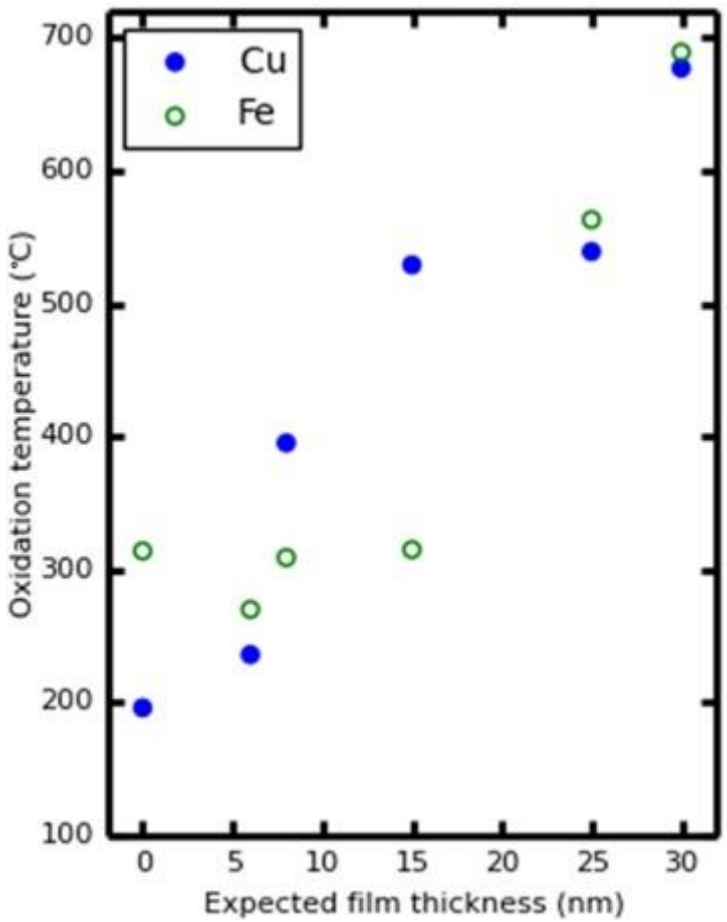

Fig. 11. Oxidation temperature in function of the expected coating thickness for the Cu (blue) and Fe powder (green).

4. Conclusion

A rotary pump-type ALD reactor was used to coat micron-sized Cu and Fe particles with Al2O3 using the TMA/H2O ALD process. It was shown that proper agitation of the powder is required to ensure a pinhole-free coating. Using SEM/EDX measurements the presence of an alumina coating was confirmed. TEM measurements illustrate the conformality and uniformity of the coating. To study the oxidation barrier properties of the coating, Cu and Fe samples with different coating thicknesses of Al2O3 were investigated with in-situ XRD and TGA. For both powders, the onset of oxidation increased with increasing coating thickness. A clear shift in oxidation temperature of 200°C was seen for the Cu sample coated with an alumina coating of 8 nm, a coating of 25 nm was required to increase the oxidation temperature for the Fe powder. This result illustrate that an alumina thin film can be an efficient oxidation barrier for micron-sized Cu and Fe powder.

Acknowledgments

The authors acknowledge financial support from the Strategic Initiative Materials in Flanders (SIM, SBO-FUNC project) and the Special Research Fund BOF of Ghent University (GOA 01G01513). J. D. acknowledges the Research Foundation Flanders (FWO-Vlaanderen) for a postdoctoral fellowship. N.C. and S.B. acknowledge financial support from European Research Council (ERC Starting Grant 335078-COLOURATOMS). The authors acknowledge S. Goeteyn for the assistance in preliminary depositions.

References

[1] A. Karimi, R. Soltani, M. Ghambari, H. Fallahdoost. *High temperature oxidation resistance of plasma sprayed and surface treated YSZ coating on Hastelloy X.* Surf. Coat. Technol., 321 (2017), pp. 378–385

[2] H. Singh, B.S. Sidhu, D. Puri, S. Prakash. *Use of plasma spray technology for deposition of high temperature oxidation/corrosion resistant coatings - A review*. Mater. Corros., 58 (2) (2007), pp. 92–102

[3] W.Q. Wang, C.K. Sha, D.Q. Sun, X.Y. Gu. *Microstructural feature, thermal shock resistance and isothermal oxidation resistance of nanostructured zirconia coating*. Mater. Sci. Eng., 424 (1-2) (2006), pp. 1–5

[4] D.C. Tsai, M.J. Deng, Z.C. Chang, B.H. Kuo, E.C. Chen, S.Y. Chang, F.S. Shieu. *Oxidation resistance and characterization of (AlCrMoTaTi)-Six-N coating deposited via magnetron sputtering*. J. Alloys Compd., 647 (2015), pp. 179–188

[5] Y.X. Xu, H. Riedl, D. Holec, L. Chen, Y. Du, P.H. Mayrhofer. *Thermal stability and oxidation resistance of sputtered Ti-Al-Cr-N hard coatings*. Surf. Coat. Technol., 324 (2017), pp. 48–56

[6] D. Longrie, D. Deduytsche, C. Detavernier. *Reactor concepts for atomic layer deposition on agitated particles: A review* J. Vac. Sci. Technol. A, 32 (1) (2014), p. 010802

[7] R.L. Puurunen. *Surface chemistry of atomic layer deposition: A case study for the trimethylaluminum/water process*. J. Appl. Phys., 97 (12) (2005)

[8] S.M. George. *Atomic Layer Deposition: An Overview*. Chem. Rev., 110 (2010), p. 111

[9] V. Miikkulainen, M. Leskelä, M. Ritala, R.L. Puurunen. *Crystallinity of inorganic films grown by atomic layer deposition: Overview and general trends*. J. Appl. Phys., 113 (2) (2013)

[10] T. Suntola. *Atomic layer epitaxy*. Mater. Sci. Rep., 4 (5) (1989), pp. 261–312

[11] M. Leskelä, M. Ritala. *Atomic layer deposition (ALD): From precursors to thin film structures*. Thin Solid Films, 409 (1) (2002), pp. 138–146

[12] R.W. Johnson, A. Hultqvist, S.F. Bent. *A brief review of atomic layer deposition: From fundamentals to applications*. Mater. Today, 17 (5) (2014), pp. 236–246

[13] J.W. Elam, D. Routkevitch, S.M. George. *Conformal Coating on Ultrahigh-Aspect-Ratio Nanopores of Anodic Alumina by Atomic Layer Deposition using sufficient reactant exposure times. Zn concentration profiles measured by EPMA following ZnO ALD showed the progressive infiltration of the ZnO ALD i*. Chem. Mater., 15 (11) (2003), pp. 3507–3517

[14] C. Detavernier, J. Dendooven, S. Pulinthanathu Sree, K.F. Ludwig, J.A. Martens. *Tailoring nanoporous materials by atomic layer deposition*. Chem. Soc. Rev., 40 (11) (2011), p. 5242

[15] J. Dendooven, K. Devloo-Casier, M. Ide, K. Grandfield, M. Kurttepeli, K.F. Ludwig, S. Bals, P. Van Der Voort, C. Detavernier. *Atomic layer deposition-based tuning of the pore size in mesoporous thin films studied by in situ grazing incidence small angle X-ray scattering*. NANOSCALE, 6 (24) (2014), pp. 14991–14998

[16] N. Avci, J. Musschoot, P.F. Smet, K. Korthout, A. Avci, C. Detavernier, D. Poelman. *Microencapsulation of Moisture-Sensitive CaS:Eu[2+] Particles with Aluminum Oxide*. J. Electrochem. Soc., 156 (11) (2009), p. J333

[17] K. Leus, J. Dendooven, N. Tahir, R. Ramachandran, M. Meledina, S. Turner, G. Van Tendeloo, J. Goeman, J. Van der Eycken, C. Detavernier, P. Van Der Voort. *Atomic Layer Deposition of Pt Nanoparticles within the Cages of MIL-101: A Mild and Recyclable Hydrogenation Catalyst*. Nanomaterials, 6 (3) (2016), p. 45

[18] C.-L. Duan, Z. Deng, K. Cao, H.-F. Yin, B. Shan, R. Chen. *Surface passivation of Fe3O4 nanoparticles with Al2O3 via atomic layer deposition in a rotating fluidized bed reactor*. J. Vac. Sci. Technol. A, 34 (4) (2016), p. 04C103

[19] L.F. Hakim, C.L. Vaughn, H.J. Dunsheath, C.S. Carney, X. Liang, P. Li, A.W. Weimer. *Synthesis of oxidation-resistant metal nanoparticles via atomic layer deposition*. Nanotechnology, 18 (34) (2007)

[20] B. Moghtaderi, I. Shames, E. Doroodchi. *Combustion prevention of iron powders by a novel coating method.* Chem. Eng. Technol., 29 (1) (2006), pp. 97–103

[21] A. Goulas, J.R. van Ommen. *Scalable production of nanostructured particles using atomic layer deposition.* Kona Powder Part. J., 31 (1) (2014), pp. 234–246

[22] H. Tiznado, D. Domínguez, F. Muñoz-Muñoz, J. Romo-Herrera, R. Machorro, O.E. Contreras, G. Soto. *Pulsed-bed atomic layer deposition setup for powder coating*. Powder Technol., 267 (2014), pp. 201–207 https://doi.org/10.1016/j.powtec.2014.07.034

[23] D. Longrie, D. Deduytsche, J. Haemers, K. Driesen, C. Detavernier. *A rotary reactor for thermal and plasma-enhanced atomic layer deposition on powders and small objects.* Surf. Coat. Technol., 213 (2012), pp. 183–191

[24] G. Rampelberg, D. Longrie, D. Deduytsche, C. Detavernier. *Plasma enhanced atomic layer deposition on powders.* ECS Trans., 64 (9) (2014), pp. 51–62

[25] W. Knaepen, C. Detavernier, R.L. Van Meirhaeghe, J. Jordan Sweet, C. Lavoie. *In-situ X-ray Diffraction study of Metal Induced Crystallization of amorphous silicon.* Thin Solid Films, 516 (15) (2008), pp. 4946–4952

[26] W. Knaepen, S. Gaudet, C. Detavernier, R.L. Van Meirhaeghe, J.J. Sweet, C. Lavoie. *In situ x-ray diffraction study of metal induced crystallization of amorphous germanium.* Journal of Applied Physics, 105 (8) (2009)

[27] G. Rampelberg, M. Schaekers, K. Martens, Q. Xie, D. Deduytsche, B. De Schutter, N. Blasco, J. Kittl, C. Detavernier. *Semiconductor-metal transition in thin VO2 films grown by ozone based atomic layer deposition.* Appl. Phys. Lett., 98 (16) (2011), p. 162902

[28] G. Rampelberg, B. De Schutter, W. Devulder, K. Martens, I. Radu, C. Detavernier. *In situ X-ray diffraction study of the controlled oxidation and reduction in the V-O system for the synthesis of VO2 and V2O3 thin films.* J. Mater. Chem. C, 3 (43) (2015), pp. 11357–11365

[29] M.D. Groner, F.H. Fabreguette, J.W. Elam, S.M. George. *Low-Temperature Al2O3 Atomic Layer Deposition.* Chem. Mater., 16 (4) (2004), pp. 639–645